Journal of Engineering and Technological Sciences

Research Paper

Corrosion Behavior of Steel 37 under Dynamic Conditions in 0.1 N H_2SO_4

Alaa Abdulhasan Atiyah & Dhuha Albusalih*

[1]Department of Materials Engineering, University of Technology, Baghdad, Iraq
[2]Al-Furat Al-Awsat Technical University, Najaf, Iraq

*Corresponding author: dhuha.kleef@atu.edu.iq

Abstract

An aggressive environment has a substantial effect on the progression of corrosion on metal surfaces and alloys. This study investigated the effect of one of the parameters that affect the corrosion process, the stirring rate, on the behavior of Steel 37 in 0.1 N of sulfuric acid. The main method used in this study is an electrochemical method (using a potentiostat at a scan rate of 3 MV.sec-1), applied at three different temperatures (25, 30, and ˚C). To evaluate the parameters of corrosion in this study, the Tafel extrapolation method was used. At a constant stirring rate, the corrosion current density was found to be increased with increasing temperature at a constant stirring rate. In addition, the corrosion rate increased with increasing stirring rate at a constant temperature due to the rise of the diffusion coefficient of oxygen. The Levich equation was used to calculate the limiting current densities, as well as the mass transfer coefficient (Km) and the Sherwood number (Sh). The Km values were calculated and it was found that the mass transfer coefficient was greater at higher temperatures and stirring rates. The results also revealed that the smallest values of Sh (2.575, 3.897) occurred at 30 °C at two stirring rates (200 and 400 rpm).

Keywords: *corrosion failure; dynamic corrosion; limiting current density; Sherwood number; static corrosion; Steel 37.*

Introduction

With steel being selected increasingly for numerous applications, failure of steel parts due to corrosion limits their usage. Particularly in aggressive environments, corrosion failure can be considered a major problem in many industrial systems. Pipe corrosion and pipe wall thinning due to pressure vessel leakage lead to equipment failure, which can have catastrophic consequences and lead to considerable economic losses. Several factors also influence the rate of corrosion development for metals and alloys, i.e., the composition of the alloy [1-8] and the product operating condition [9-11]. In addition, the environmental hostility degree, which includes the liquid flow, protective measures, and service life of the product, has also been considered [8]. Flow corrosion results in rapid premature failure of materials when compared to static corrosion if both are in contact with a corrosive environment. Work has been carried out to study the effect of flow on mild steel erosion–corrosion behavior in several corrosive conditions, including acidity, alkalinity, and neutral solutions with corrosive CO_2 gas or erosion particles [12]. Relative motion between the environment and the surface of the metal causes modification of the metal surface corrosion rate. This phenomenon is chiefly evident in the difficulty of applying the results of static corrosion testing alone to the selection of fabrics for the construction of chemical process equipment.

A sequence of simultaneous processes occurs during corrosion, which include physical, chemical, and electrochemical transport on the metal's surface during anodic and cathodic polarization. These involve metal dissolution, passive film formation, the evolution of hydrogen, and the reduction of oxygen. The first of the three processes requires ionic movement within the liquid phase to and/or from the metal surface under the influence of the electrical potential gradient. The oxygen reduction reaction requires the diffusion of oxygen molecules down a chemical potential gradient. The overall electrochemical behavior of the metal is difficult to elucidate from electrochemical experiments in a stationary solution alone, but it may be ascertained with more confidence by the introduction of flow [13]. Moreover, it is important to mention that the velocity of the fluid plays an

ISSN: 2337-5779
J. Eng. Technol. Sci. Vol. 55, No. 6, 2023, 639-646
DOI: 10.5614/j.eng.technol.sci.2023.55.6.2

essential role in increasing the metal corrosion rate, whereas at higher velocities it may become independent of this parameter. However, as the speed is further increased, the reduction reaction eventually becomes totally activation-controlled. Consequently, the reaction rate becomes independent of velocity at very high velocities [13].

Several studies have been conducted on the mass transfer with the current conditions and corrosion [14-18], while other studies examined flow-accelerated corrosion (FAC) [19-24]. Both the rotating disc electrode (RDE) and the rotating cylinder have been effectively implemented in the laboratory to study the flow effect on the rate of corrosion. They are much faster to use than actual pipelines and other real geometries. Several studies used RDE in electrochemistry to examine the metal dissolution kinetics under dynamic laboratory conditions [25-30]. Ethirajulu *et al.* [33] considered CO_2 corrosion prediction in pipe flow under $FeCO_3$ scale-forming conditions. Donghong Z. *et al.* [31] examined the impact of hydrodynamics on the boundary layer and the diffusion boundary layer in the near wall zone on gas–liquid two-phase-flow-prompted corrosion in pipelines. The study also took into account the hydrodynamic effect of fully developed gas–liquid slug flow in an upward tube with limiting diffusion current probes. In addition, conductivity probes and digital high-speed video systems were studied. The study considered both the shear stress and the mass transfer coefficient, particularly in the near-wall zone. It was found that all increase with the rise of the superficial gas velocity and decrease with the improvement of the superficial liquid velocity. In addition, the local void fraction of the slug unit and the liquid slug increases when the superficial gas velocity increases.

Temperature variation plays an important role in metal product corrosion development processes, equipment, and structures. This can be related to the effects of the rate of all chemical reactions. Few studies have been implemented to study the effect of temperature on the corrosion rate of steel. Recent research on iron-carbon alloys in 0.1 N solution suggested that temperature plays an important role in the corrosion progress processes for the surface of metals and alloys [8]. The authors suggest a considerable effect at different temperatures. The corrosion rate parameters for the iron–carbon system in 0.1 N solution were calculated at different temperatures. The study claimed that a temperature increase of 10 °C results in an acceleration of the dissolution of the iron carbon by approximately 2.3 times. Accordingly, the dissolution of the metal accelerates as a result. The work also proposed that corrosion increases in iron–carbon alloys with high carbon contents.

The current study addressed the influence of dynamic conditions at 200 and 400 rpm for corrosion of Steel 37 in 0.1 N H_2SO_4 solution at three temperatures to evaluate the mass transfer coefficients and the Sherwood numbers.

Experimental Procedure

Material and Chemicals

Steel 37 was used in this work. The used material was cut into a cylindric shape with dimensions of 10 x 10 x 3 mm and it was mounted using a Qx-Machine Inlay hot mounting device (manufactured in China). Mounting was carried out by formaldehyde (bakelite) at 138 ℃ for 8 minutes. Mounting was conducted by leaving the specimen's upper side exposed with a surface area of 1 cm^2. In electrochemical studies, suitable provisions were made on the side for electrical contact. Subsequently, the mounted samples were wet-grounded with silicon carbide papers of varying degrees (600, 800, 1000, and 1200). During grinding, all samples were rotated 90° for each degree of grinding paper. The samples were polished using a Ma-Pao 160E Grinder and Polisher machine (manufactured in China), by using a cloth and alumina slurry with 0.3 µm particle size. The specimens were polished and washed with water, degreased with methanol, and used for electrochemical tests.

The basic solution was 0.1 N H_2SO_4 (98%). All experiments were conducted at three different temperatures 25, 30, and 35℃. Stirring speeds were applied at 200 and 400 rpm with a Digital Magnetic Stirrer/Hotplate Stirrer/Hot plate from Daihan Labtech Co., Ltd.

Instruments

The polarization study in this work was carried out in a Winking M Lab 200 Potentiostat from Bank-electronic using an electrochemical standard cell. Electrochemical measurements were conducted by using a potentiostat by SCI electrochemical software at a scan rate of 3 mV.sec-1. The studies were started when the open circuit potential (Eoc) change was less and more than 200 mV average. Two chief measurements were considered: corrosion potential (Ecorr) and corrosion current density (icorr) additional to the Tafel slope measurement.

Results and Discussions

Figure 1 shows the variation of potential with time for Steel 37 in 0.1 N sulphuric acid under static and dynamic conditions at 200 and 400 rpm. This figure indicates a small change, i.e., about 20, in the potential under dynamic conditions.

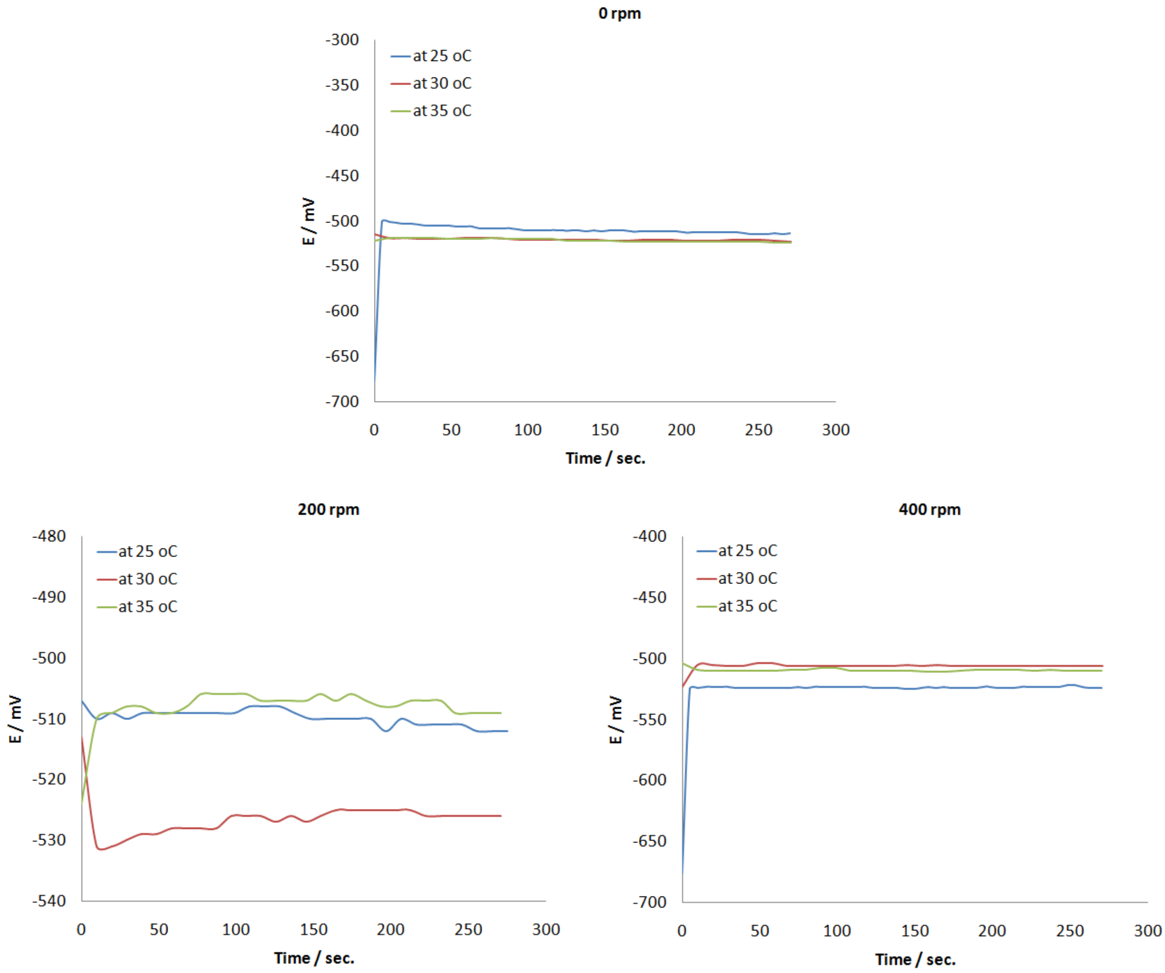

Figure 1 Potential–time measurements of Steel 37 in 0.1 N H_2SO_4 solution under dynamic conditions.

Figure 2 shows the Tafel plots of Steel 37 in 0.1 N sulphuric acid at three temperatures under static and dynamic conditions. Stirring was used to improve the convection in the metal surface neighborhood. Another reason for using stirring is to lower the thickness of the diffusion boundary layer and to supply the cathodic reactant, i.e., oxygen, at a higher rate. The oxygen reduction, therefore, comes to be a more facile process. The corrosion parameters are listed in Table 1, representing the increase of corrosion current density with increasing temperature at a constant stirring rate. The table also shows an increase in the current densities with the improvement of the stirring rate of the medium at a constant temperature. The temperature impacts the corrosion rate for metals fundamentally by affecting factors that control the oxygen rate diffusion.

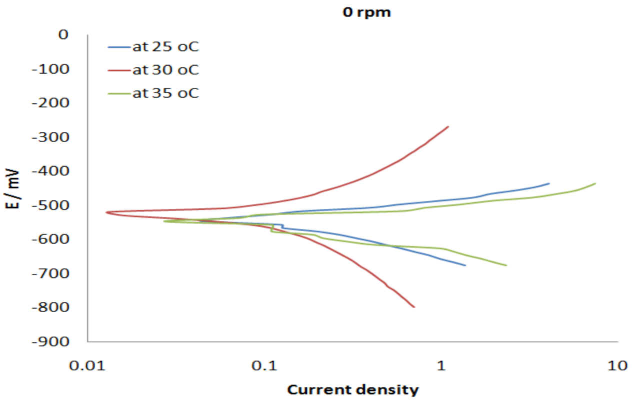

Tafel plots of Steel 37 in 0.1 N H_2SO_4 solution under 0 rpm dynamic conditions.

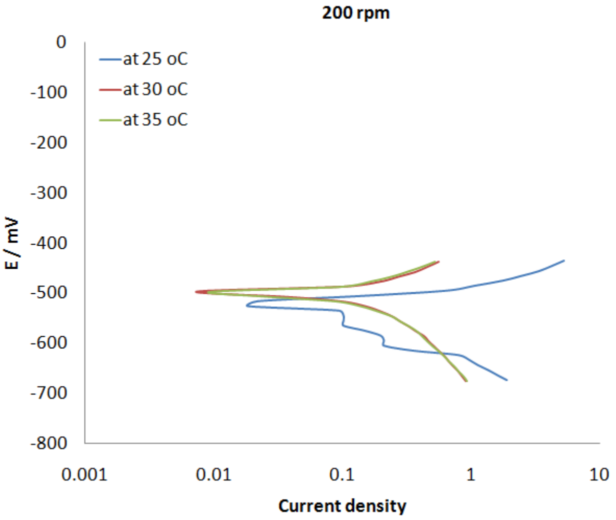

Tafel plots of Steel 37 in 0.1 N H_2SO_4 solution under 0 rpm dynamic conditions.

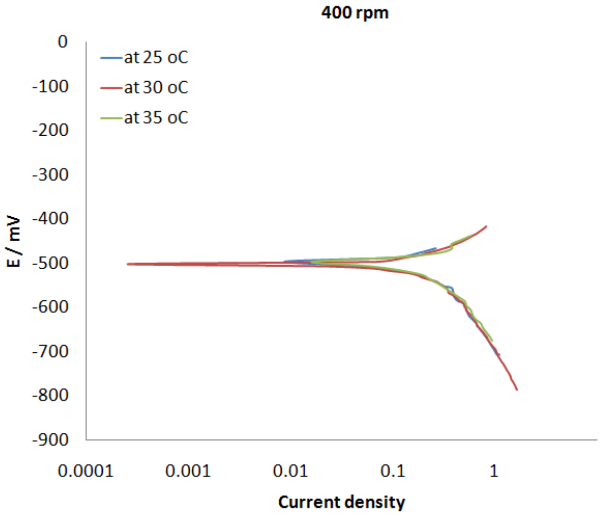

Tafel plots of Steel 37 in 0.1 N H_2SO_4 solution under 400 rpm dynamic conditions.

Figure 2 Tafel plots of Steel 37 in 0.1 N H_2SO_4 solution in 0, 200 under 400 rpm dynamic conditions.

Table 1 Corrosion parameters of Steel 37 in 0.1 N H_2SO_4 solution at three temperatures and two stirring speeds.

Speed	Temp. c°C	E_{oc} mV	E_{corr} mV	i_{corr} µA.cm^{-2}	$-b_c$ mV.dec^{-1}	$+b_a$ mV.dec^{-1}
0	25	-514	-544.7	68.44	73.2	50.4
	30	-523	-520.9	71.68	205.7	130.1
	35	-524	-545.6	83.27	144.6	44.7
200	25	-512	-524.2	80.96	106.7	38.4
	30	-526	-497.6	112.73	151.7	80.9
	35	-509	-497.9	141.38	190.2	108.2
400	25	-523	-495.8	81.19	93.5	59.5
	30	-506	-501.7	119.46	120.0	83.3
	35	-510	-496.5	220.25	259.9	150.7

On the other hand, the velocity mainly affects the rate of corrosion by influencing the diffusion phenomena. When the velocity affects the limiting diffusion current, this is considered to be a function of the physical geometry of the system. In addition, the diffusion process is affected by the velocity when the flow conditions are laminar compared to the turbulence availability. The maximum flux of a species can be derived by the Levich equation to a unit area of the electrode surface under laminar flow. For a particular species, under isothermal conditions:

$$i_L \alpha \omega^{0.5} \tag{1}$$

The theoretical value of the limiting current density (iL) for the oxygen reduction reaction can be evaluated from the kinematics viscosity (υ), the fluid angular velocity (ω), the diffusion coefficient (D), and the concentration of oxygen (the electroactive species) (Cb) using the Levich equation [16], as follows:

$$i_L = 0.62F\omega^{0.5}D^{0.667}\upsilon^{-0.166}C_b \tag{2}$$

Eqs. (1) and (2) are usually applied to the analysis of the mass transfer controlled cathodic process and Eq. (2) predicts a linear dependence of the limiting current density on (ω0.5). Moreover, the extrapolated line should pass through the origin of the coordinate system, as shown in Figure 3.

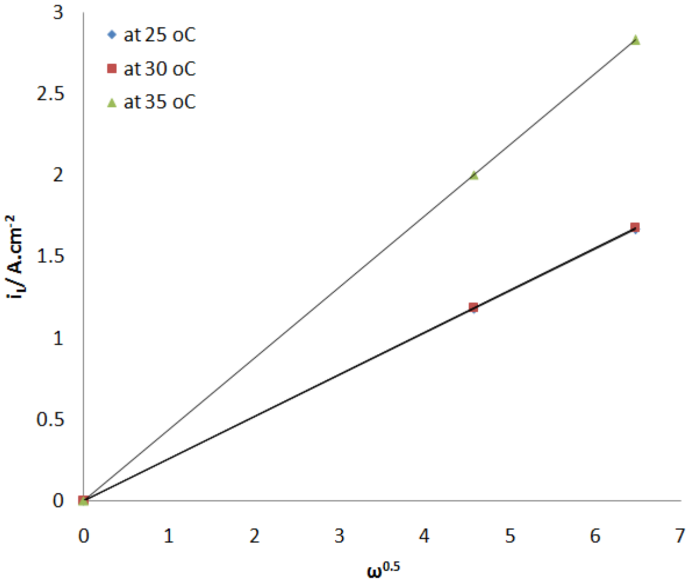

Figure 3 Limiting current density of the oxygen reduction versus ω0.5 at different temperatures for Steel 37 in 0.1 N H_2SO_4 solution under dynamic conditions.

The limiting current density was calculated at three temperatures for the four-electron process mechanism of the oxygen reduction reaction at various stirring rates. The results are tabulated in Table 2.

Table 2 Limiting current density of Steel 37 in 0.1 N H_2SO_4 under dynamic conditions.

rpm	ω	$ω^{0.5}$	i_L/ A.cm^{-2} 25°C	 30 °C	 35°C
200	20.93333	4.575296	1.178	1.185	2.003
400	41.86667	6.470446	1.666	1.676	2.832

The coefficient of mass transfer Km can be calculated approximately using Eq.(3):

$$K\_m=i\_L/(zFC\_b) \quad (3)$$

where z is the transferred charge (= 2), F is the Faraday constant, and Cb is the oxygen concentration. The Km values are listed in Table 3. They increased as the stirring rate increased. At a constant stirring rate, Km also increased with increasing temperature.

Table 3 Values of the mass transfer coefficient and Sherwood number.

rpm	Temp./°C	K_m x 10^{-6}	Sh. No. x10^3
200	25	4.73	2.815
	30	5.25	2.757
	35	9.27	4.308
400	25	6.69	3.982
	30	7.42	3.897
	35	13.1	6.087

An improvement in iL values is considered to be a result of the increase in stirring and temperature. This results in an improvement in the oxygen flux that arrives at the surface and decreases in the resistance that restricts the oxygen transfer.

The mass transfer coefficient (Km) value can often be correlated with the dimensionless quantities Reynolds number (Re) and Schmidt number (Sc). The mass transfer coefficient is expressed in terms of the Sherwood number (Sh) as shown in Eq. (4) [32].

$$Sh = (K\_m\ d)/2D \quad (4)$$

where D is the diffusion coefficient, and d is the disc diameter (2.5 cm). The Sherwood numbers are listed in Table 3. The smallest value of Sh was at 30 °C at a constant stirring rate. This confirms the Tafel plot shifting to lower values of current densities in Figure 1 at 30 °C.

Conclusions

The results of this study indicate a minor change in the potential variation with dynamic conditions in 0.1 N sulphuric acid. There was an increase in the corrosion current density with increasing temperature at a constant stirring rate. There was an increase in the current densities with increasing stirring rate of the medium at a constant temperature. The results also showed that the temperature changes the metal corrosion rate mainly by prompting factors that control the oxygen diffusion rate. Finally, as the temperature rises, the diffusion coefficient of oxygen also increases, which tends to improve the rate of corrosion.

References

[1] Konovalova, V., *The Effect of Temperature on the Corrosion Rate of Iron-carbon Alloys,* Materials Today: Proceedings, **38**, pp. 1326-1329, 2001.

[2] Little, B., Wagner, P. & Mansfeld, F., *Microbiologically Influenced Corrosion of Metals and Alloys,* International Materials Reviews, **36**(1), pp. 253-272, 1991.

[3] Giggins, C.S. & Pettit, F.S., *Corrosion of Metals and Alloys in Mixed Gas Environments at Elevated Temperatures,* Oxidation of Metals, **14**, pp. 363-413,1980.

[4] Tomashov, N.D., *Development of the Electrochemical Theory of Metallic Corrosion*, Corrosion, **20**(1), pp. 7t-14t, 1980.

[5] Al-Hassan, S., Mishra, B., Olson, D.L. & Salama, M.M.*, Effect of Microstructure on Corrosion of Steels in Aqueous Solutions Containing Carbon Dioxide*.,Corrosion, **54**(6), pp. 490-491, 1980.

[6] Shreir, L.L. (ed.), *Corrosion: Metal/Environment Reactions,* London, Newnes, 2007.

[7] Lopez, D.A., Perez, T. & Simison, S.N., *The Influence of Microstructure and Chemical Composition of Carbon and Low Alloy Steels in CO_2 Corrosion, A State-of-the-art Appraisal*, Materials & Design, **24**(8), pp. 561-575.2003.

[8] Kawahara, Y., *High-temperature Corrosion Mechanisms and Effect of Alloying Elements for Materials used in Waste Incineration Environment,* Corrosion Science, **44**(2), pp. 223-245.2002.

[9] Scully, J.R., Inman, S.B., Gerard, A.Y., Taylor, C.D., Windl, W., Schreiber, D.K., Lu, P., Saal, J.E. & Frankel, G.S., *Controlling the Corrosion Resistance of Multi-principal Element Alloys,* Scripta Materialia, **188**, pp. 96-101.2020.

[10] Akpanyung, K.V. & Loto, R.T., *Pitting Corrosion Evaluation: A Review,* Journal of Physics: Conference Series **1378**(2), 022088, IOP Publishing, 2019.

[11] Abbas, M. & Shafiee, M., *An Overview of Maintenance Management Strategies for Corroded Steel Structures in Extreme Marine Environments,* Marine Structures, **71**, 102718, 2020.

[12] Brownlie, F., Hodgkiess, T., Pearson, A. & Galloway, A.M., *A Study on the Erosion-corrosion Behaviour of Engineering Materials Used in the Geothermal Industry,* Wear, **477**, 203821, 2021.

[13] Yerokhin, A., Mukaeva, V.R., Parfenov, E.V., Laugel, N. & Matthews, A., *Charge Transfer Mechanisms underlying Contact Glow Discharge Electrolysis.* Electrochimica Acta, **312**, pp. 441-456. 2019.

[14] Zhao, J., Tu, Z. & Chan, S.H., *Carbon Corrosion Mechanism and Mitigation Strategies in a Proton exchange membrane fuel cell (PEMFC): A review.* Journal of Power Sources, **488**, p.229434. 2021.

[15] Angst, U.M., *Predicting the Time to Corrosion Initiation in Reinforced Concrete Structures Exposed to Chlorides.* Cement and Concrete Research, **115**, pp. 559-567. 2019.

[16] Hernández, H.H., Reynoso, A.M.R., González, J.C.T., Morán, C.O.G., Hernández, J.G.M., Ruiz, A.M., Hernández, J.M. & Cruz, R.O., *Electrochemical Impedance Spectroscopy (EIS): A Review Study of Basic Aspects of the Corrosion Mechanism Applied to Steels.* Electrochemical Impedance Spectroscopy, pp. 137-144.2020.

[17] Wahyudi, S., Gapsari, F. & Awali, H., *Optimization of Chemical Environment Condition towards Corrosion Rate of Sulfuric Acid Resistant Alloy Metal (saramet) using Response Surface Methodology*, Appl. Mech. Mater., **493**, pp. 733-738, 2014.

[18] Wang, Q.Y., Bai, S.L. & Liu, Z.D., *Surface Characterization and Erosion–corrosion Behavior of Q235 Steel in Dynamic Flow.* Tribology Letters, **53**(1), pp. 271-279, 2014.

[19] Fontana, M.G. & Green, N.D., Corrosion Engineering 2nd ed., McGraw Hill, 1963.

[20] Keating, A. & Nesic, S., *Prediction of Two-phase Erosion-corrosion in Bends*, Second International Conference on CFD in the Minerals and Process Industries CSIRO, Melbourne, Australia, 6-8 December 1999.

[21] Wang, H., Vedapuri, D., Cai,J.Y., Hong, T. & Jepson, W.P., *Mass Transfer Coefficient Measurement in Water/Oil/Gas Multiphase Flow*, J. Energy Resour. Technol., **123**(2), pp.144-149, June 2001.

[22] Rizk, T.Y., Thompson, G.E. & Dawson, J.L., *Mass Transfer Enhancement Associated with Sudden Flow Expansion*, Corrosion and Protection Center, **38**(10), pp. 1801-1814, , October 1996.

[23] Al-Darbi, M.M., Nouri, A., Islam, M.R. & Jaralla, A.A., *The Inhibitive Characteristics of Mixed Inhibitor Combinations Under Heat and Mass Transfer Conditions*, Energy Sources, Part A: Recovery, Utilization, and Environmental Effects, **24**(11), pp. 1019-1030, November 2002.

[24] Liu, C.-B. & Zheng, Y.-G., *Research Progress on Modeling and Numerical Simulation of Flow – Accelerated – Corrosion*, Corrosion Science and Protection Technology, **20**(6), pp. 436-439, Nov.2008.

[25] Uchida, S., Naitoh, M., Okada, H., Uehara, Y., Koshizuka, S., Svoboda, R. & Lister, D.H., *Effects of Water Chemistry on Flow Accelerated Corrosion and Liquid Droplet Impingement Accelerated Corrosion*, Power Plant Chemistry, **11**(12), pp. 704-717, 2009.

[26] Efird, K.D., *Jet Impingement Testing for Flow Accelerated Corrosion*, Paper presented at CORROSION 2000, March 26 - 31, 2000.

[27] Liu, G., Tree, D.A. & High, M.S., *Relationships Between Rotating Disk Corrosion Measurements and Corrosion in Pipe Flow*, Corrosion, **50**(08), pp. 584-593, August 1994,

[28] Efird, K.D., Wright, E.J., Boros, J.A. & Hailey, T.G., *Correlation of Steel Corrosion in Pipe Flow with Jet Impingement and Rotating Cylinder Tests*, Corrosion Engineering,**49**(12), pp. 993-1003, 1992.

[29] Efird, K.D., Wright, E.J., Boros, J.A. & Hailey, T.G., *Correlation of Steel Corrosion in Pipe Flow with Jet Impingement and Rotating Cylinder Tests*, Corrosion, **49**(12), NACE-93120992, 1993.

[30] Augustin, C.O. & Cyril, A., *Corrosion of Rotating Magnesium Electrode in Neutral Electrolytes*, JCSE, **5**, Preprint 8.

[31] Nesic, S., Solvi, G.T. & Enerhaug, J., *Comparison of the Rotating Cylinder and Pipe Flow Tests for Flow-Sensitive Carbon Dioxide Corrosion,* Corrosion, **51**(10), pp.773-786, 1995.

Manuscript Received: 27 May 2023
Revised Manuscript Received: 26 December 2023
Accepted Manuscript: 28 December 2023